

What can we learn from gravitational waves from nearby core-collapse supernovae?

This content has been downloaded from IOPscience. Please scroll down to see the full text.

2015 J. Phys.: Conf. Ser. 600 012009

(<http://iopscience.iop.org/1742-6596/600/1/012009>)

View [the table of contents for this issue](#), or go to the [journal homepage](#) for more

Download details:

IP Address: 131.169.4.70

This content was downloaded on 01/03/2016 at 22:57

Please note that [terms and conditions apply](#).

What can we learn from gravitational waves from nearby core-collapse supernovae?

Yudai Suwa^{1,2}, Takaaki Yokozawa³, Mitsuhiro Asano³, Tsubasa Kayano⁴, Nobuyuki Kanda³, Yusuke Koshio⁴, and Mark R. Vagins^{5,6}

¹Yukawa Institute for Theoretical Physics, Kyoto University, Oiwake-cho, Kitashirakawa, Sakyo-ku, Kyoto, 606-8502, Japan

²Max-Planck-Institute für Astrophysik, Karl-Schwarzschild-Str. 1, 85748 Garching, Germany

³Graduate School of Science, Osaka City University, Sumiyoshi-ku, Osaka 558-8585, Japan

⁴Department of Physics, Okayama University, Okayama, Okayama, 700-8530, Japan

⁵Kavli Institute for the Physics and Mathematics of the Universe(WPI), Todai Institutes for Advanced Study, University of Tokyo, Kashiwa, Chiba 277-8583, Japan

⁶Department of Physics and Astronomy, University of California, Irvine, Irvine, CA 92697-4575, USA

E-mail: suwa@yukawa.kyoto-u.ac.jp

Abstract.

Core-collapse supernova is one of the expected sources of gravitational wave (GW). The GW detection can be a smoking gun to probe the still unknown explosion mechanism. In the coming era of “multi-messenger astronomy”, we can use photons, neutrinos and GW simultaneously to investigate these objects. By performing multi-dimensional simulations of neutrino-radiation hydrodynamics systematically, we calculate the gravitational wave and neutrino signals from nearby (galactic) core-collapse supernova. Based on these signals we will discuss the extractable information about the very central part of core-collapse supernovae.

1. Introduction

Since there are various types of physics involved in core-collapse supernova explosions, detailed numerical simulations are indispensable. For instance, gravity describes how the matter collapses and how much energy is released during the collapse. In addition, a final outcome of supernovae are neutron stars (NSs), so that the nuclear force, which determines the structure of a NS, is critically important. Neutrino interaction rates, which give the cooling rates of the core as well as heating rates of post-shock material by neutrino absorption (this will be explained later), are treated in great detail to give a quantitatively correct answer. This is because the total amount of neutrino emission is $\sim 10^{53}$ erg, while the explosion energy itself is $\sim 10^{51}$ erg, therefore only a few percent of energy deposition by neutrinos can drive the explosion; indeed, this is the so-called standard scenario of core-collapse supernovae (see [1] for original idea and [2, 3, 4] for recent reviews). The electromagnetic interaction also plays an important role because the system consists of fully-ionized plasma, and so Coulomb scattering allows us to treat the stellar matter as if it were in the fluid state.

Since such complex phenomena are difficult to model by analytic calculations, we need to perform detailed numerical computations including all relevant physical interactions. Ever since



the first pioneering numerical simulation was done by Colgate & White in 1966 [5], many scientists have put continuous efforts on producing the realistic explosion for almost 50 years, but yet nobody has succeeded, even by using supercomputers.

Not only the fact that all interactions involve the phenomena makes the system more complex, but it also makes them observable in various ways. This is because these interactions cause their own kind of emission (electromagnetic waves, neutrinos, gravitational waves, and cosmic rays) so that they can be seen with various kind of signals (particles and waves), which is called “multi-messenger astronomy”. It should be noted that these signals are generated at different places due to different coupling constants with matter of the governing interactions. Hence, if an event occurs, we can get some information from different locations in the exploding stars using different signals (tomography). In addition, we can use this information from different epochs of the different times. This character makes it possible to follow up by different ways once we observe the early phase of explosion in any manner. Therefore, we can see these cosmic explosions using multi-messenger time domain astronomical observations.

In this study, we aim to develop a new strategy to give a constraint on the rotation of the core using GW and neutrino observations.

2. Hydrodynamical Simulations of Supernovae

The numerical methods used in this study are the same as [6, 7, 8, 9, 10]. In this code, we solve neutrino radiation hydrodynamic equations, which consist of hydrodynamic equations and neutrino radiative transfer equation (see [8] for more details). The nuclear equation of state [11] with the incompressibility parameter of $K = 220$ MeV. As for the initial condition, we employ $11.2M_{\odot}$ model from [12], which was used in several previous works.

The rotation is imposed with shellular rotation law as

$$\Omega(r) = \Omega_0 \frac{r_0^2}{r^2 + r_0^2}, \quad (1)$$

where $\Omega(r)$ is an angular velocity with r being the radius from the center, Ω_0 is the angular velocity at the center, and r_0 is a radius that determines the degree of differential rotation. Here, we employ $r_0 = 1000$ km. In order to investigate how the rotation affects emissions of gravitational waves and neutrinos, we perform simulations with different rotation strengths of $\Omega_0 = 0.0 \pi$ and 1.0π radian s^{-1} .

In this study, we evaluate the gravitational wave emission from aspherical motion of fluids via the Newtonian quadrupole formulae of [13]. We do not discuss the gravitational wave emission from anisotropic neutrino emission [14, 15, 16] because this component contributes to GW at later time and does not affect GW around the bounce time.

The left panel of Figure 1 represents the time evolution of luminosities of electron-type neutrinos (ν_e). One can see the general trend does not depend on the initial rotation rate very much. In the first few tens of ms for ν_e , there is the so-called neutronization burst, which is generated by the rapid absorption of electrons by protons (electron capture; $e + p \rightarrow n + \nu_e$) in the regime between the shock and protoneutron star, causing emission of large amounts of ν_e . After that the neutrino luminosity is gradually decreasing, but a large luminosity is still observed. It is found that the fast rotation model ($\Omega_0 = 1.0\pi$ rad s^{-1}) results in slightly smaller luminosity due to stronger centrifugal force and slower contraction of the PNS, while slower rotation models share similar, minimally-affected characteristics as compared to the non-rotating case. Therefore, we can argue that the currently employed rotation strength does not significantly change the generic picture about neutrinos.

The right panel of Figure 1 depicts the time evolution of the gravitational wave signal. Note that in the early phase the gravitational wave strength strongly depends on the initial

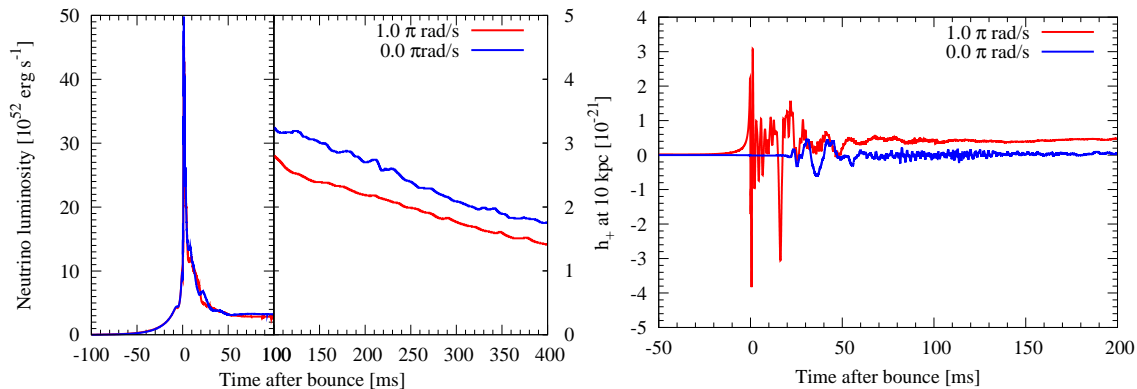


Figure 1. (*Left*): Time evolution of luminosities of electron-type neutrinos (ν_e). Each line represents models with different initial rotation rates, i.e., no rotation ($\Omega_0 = 0.0\pi$) (blue) and $\Omega_0 = 1.0\pi$ rad s⁻¹ (red), respectively. (*Right*): GW amplitude as a function of time for a core-collapse supernova occurring 10 kpc from the observer. The fast rotation model exhibits a large amplitude GW at the bounce, while the slow rotation models have very small amplitudes. Since the later phase (i.e., a few tens of ms after the bounce) activity is dominated by convection motion, all models imply similar amplitude in the later phase.

rotation. As for models without rotation, the density structure is almost spherically symmetric so that there is no or only small GW emission. On the other hand, the strongly rotating model exhibits strong GW emission at the time of bounce because the centrifugal force makes the core asymmetric. Therefore, we can constrain the rotation strength by detecting GW at just the time of bounce. We can constrain the bounce time in turn using neutrino data as shown in the left panel, in which we show that the neutrino emission does not depend on the rotation strength so that neutrinos are a guaranteed signal from core-collapse supernova.

3. Detector Simulations and Detectabilities

In the following, we explain the detector simulations for KAGRA (GW detector) and EGADS (neutrino detector). The detail of the simulations and data analysis can be found in [17].

One of the important benefits of employing EGADS and KAGRA is the close proximity of these two detectors. This makes it possible to avoid any significant time-lag in arrival times of gravitational wave and neutrino signals due to distance between the detectors. Since both gravitational wave interferometers and Water Cherenkov neutrino detectors have much worse angular resolution than that of optical telescopes, the correction of arrival time based on direction for well-separated detectors will have a larger error than the timing accuracy which is required in this study, < 1 msec, for neutrino and gravitational wave signals only. Closely placed detectors do not suffer from this problem.

At first, we consider GW. To evaluate signal and noise power from obtained $s_{det}(t)$, the Excess Power Filter [18] and Short Time Fourier Transform (STFT) are used. The simulated signal is whitened via a FIR whitening filter to flatten the noise spectrum in the frequency domain. The whitened signal $\tilde{S}_w(f)$ is calculated by

$$\tilde{S}_w(t_s, f) = \frac{\tilde{S}(t_s, f)}{\langle \tilde{N}(f) \rangle}, \quad (2)$$

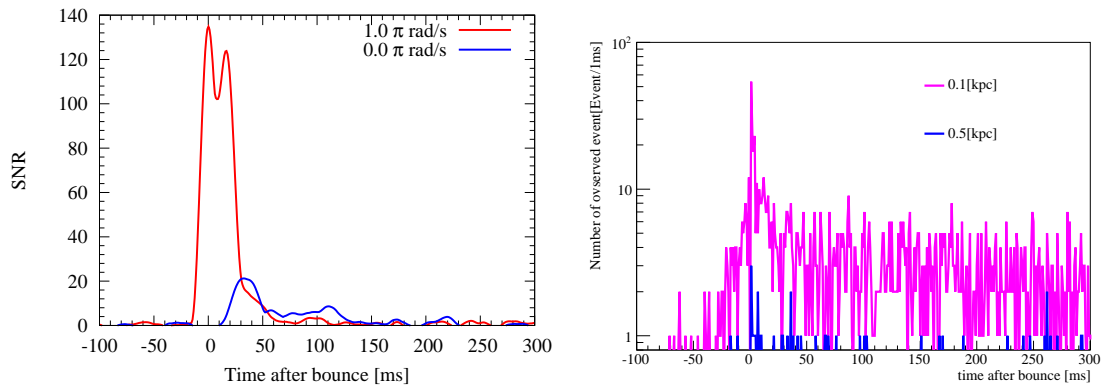


Figure 2. (*Left*): Time variation of obtained SNR. Each color shows one progenitor core rotation model, 0.0π (blue) and 1.0π (red) rad s^{-1} , respectively. The supernova distance is set to 1.0 kpc and on-direction for the KAGRA detector. (*Right*): Fluctuations of observed number of neutrinos for the distance 0.1 kpc (red) and 0.5 kpc (blue). The $1.0 \pi \text{rad s}^{-1}$ model is used for this figure.

and $\tilde{S}(t_s, f)$ is calculated by

$$\tilde{S}(t_s, f) = \int_{t_s}^{t_s + \Delta t} s_{det}(t') W(t' - t_s) \exp(-2\pi i f t') dt', \quad (3)$$

where $\langle \tilde{N}(f) \rangle$ is obtained from the running median of simulated noise data, and $W(t)$ is a Hann window function. The signal power P_s and Signal to Noise Ratio (SNR) can be defined as follows:

$$P_s(t_s) = \sqrt{\frac{\int \tilde{S}_w^*(t_s, f) \cdot \tilde{S}_w(t_s, f) df}{\int \langle \tilde{N}_w^*(f) \cdot \tilde{N}_w(f) \rangle df}}, \quad (4)$$

$$SNR(t_s) = \frac{P_s(t_s) - m}{\sigma}, \quad (5)$$

where m and σ are the normalized mean and deviation of $P_n = \sqrt{\int \tilde{N}_w^*(f) \cdot \tilde{N}_w(f) df}$ distribution, respectively. To obtain m and σ we first evaluate the noise behavior, without injecting a supernova signal, and evaluate P_n . The noise distribution shows $m=1$ and $\sigma=0.06$. The left panel of Figure 2 shows one example of the time variation of obtained SNR for each rotation model. The supernova distance is set to an on-direction 1.0 kpc for the KAGRA detector.

Next, we consider neutrinos. Using numerical results of neutrinos shown in the previous section and detector sensitivity, we evaluate the numbers of neutrons detectable by EGADS. The right panel of Figure 2 shows the expected number in EGADS for a supernova explosion near the center of our galaxy with $\Omega_0 = 1.0 \pi \text{ rad s}^{-1}$.

Based on these two detector simulations, we investigate the method of how to determine progenitor core rotation from these detectors. The analysis path is as follows: (i) Run supernova detection simulation with KAGRA and EGADS detector, respectively. (ii) Extract the epoch time of GW, \mathcal{T}_{GW} , and neutronization burst, \mathcal{T}_ν . (iii) Compare these times and determine rotation or not. (iv) Loop 10,000 times and evaluate P_r , which is the probability to of core rotation. The initial angular momentum of progenitor core rotation in the supernova models are given several different magnitudes: $\Omega_0 = 0.0 \pi$ and $1.0 \pi \text{ rad s}^{-1}$. The distance to the SN

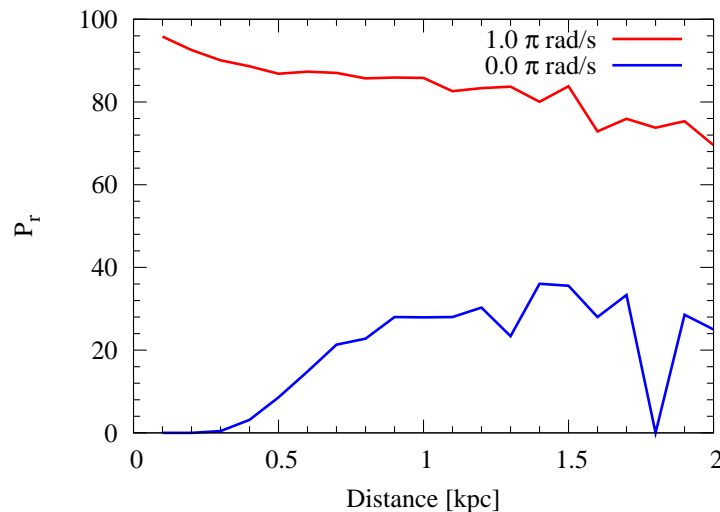


Figure 3. Model dependence of P_r distribution, which is the probability of core rotation. Horizontal axis shows distance. Each color shows one progenitor core rotation model, 0.0π (blue) and 1.0π (red) rad s^{-1} , respectively.

is chosen to be uniformly distributed between 0.1 to 2.0 kpc. The incident direction strongly affects GW detector response, but has little bearing on neutrino detection.

Figure 3 shows the distance dependence of P_r for each progenitor core rotation model, where P_r is defined as the probability of core rotation when both GW and neutronization burst signals have been observed. Once again, each color represents different progenitor core rotation models, 0.0π (blue) and 1.0π (red) rad s^{-1} , respectively. We have obtained these conclusions: (1) For weakly rotating models, the P_r value is expected to be close to 0%. In the near distance cases (0.1 and 0.2 kpc) the P_r value is almost 0 as expected. But in the far distance (>0.5 kpc) the P_r value becomes larger because of growing statistical uncertainty on the number of observed events, which leads in turn to reduced determination accuracy of the neutronization burst time (\mathcal{T}_ν). (2) For the strongly rotating model ($1.0 \pi \text{ rad s}^{-1}$), the P_r value is as expected close to 100%. But, there are two peaks due to mis-identifying \mathcal{T}_{GW} . This makes for a lower P_r for the far distance. Still, even for the 2.0 kpc case the P_r value exceeds 70%.

4. Summary

By using a consistent supernova explosion model emitting both GWs and neutrinos, we investigate the progenitor core rotation to compare the GW emission start time, \mathcal{T}_{GW} , obtained from KAGRA detector, and neutronization burst time, \mathcal{T}_ν , which is obtained from EGADS detector. The results show if a nearby supernova is very close (<0.2 kpc), we can correctly determine no core rotation about 100% of the time if the progenitor core is indeed not rotating, and determine the presence of core rotation about 90% if the progenitor core is strongly rotating. Note that we investigated only nearby supernovae using only a single GW and neutrino detector for this analysis. For more detail, see [17].

Acknowledgments

This work was supported by the MEXT Grant-in-Aid for Scientific Research on Innovative Areas “New Developments in Astrophysics Through Multi-Messenger Observations of Gravitational Wave Sources” (Nos. 24103004, 24103005, 24103006, 25103511), JSPS postdoctoral fellowships

for research abroad, MEXT SPIRE, and JICFuS. Numerical computations in this study were in part carried on XC30 at CfCA in NAOJ and SR16000 at YITP in Kyoto University.

- [1] Bethe H A and Wilson J R 1985 ApJ **295** 14–23
- [2] Kotake K, Takiwaki T, Suwa Y, Iwakami Nakano W, Kawagoe S, Masada Y and Fujimoto S i 2012 *Advances in Astronomy* **2012** 428757 (*Preprint* 1204.2330)
- [3] Janka H T 2012 *Annual Review of Nuclear and Particle Science* **62** 407–451 (*Preprint* 1206.2503)
- [4] Burrows A 2013 *Reviews of Modern Physics* **85** 245–261 (*Preprint* 1210.4921)
- [5] Colgate S A and White R H 1966 ApJ **143** 626
- [6] Suwa Y, Kotake K, Takiwaki T, Whitehouse S C, Liebendörfer M and Sato K 2010 PASJ **62** L49–L53
- [7] Suwa Y, Kotake K, Takiwaki T, Liebendörfer M and Sato K 2011 ApJ **738** 165–+ (*Preprint* 1106.5487)
- [8] Suwa Y, Takiwaki T, Kotake K, Fischer T, Liebendörfer M and Sato K 2013 ApJ **764** 99 (*Preprint* 1206.6101)
- [9] Suwa Y 2014 PASJ **66** L1 (*Preprint* 1311.7249)
- [10] Suwa Y, Yamada S, Takiwaki T and Kotake K 2014 *ArXiv e-prints* (*Preprint* 1406.6414)
- [11] Lattimer J M and Swesty F D 1991 *Nuclear Physics A* **535** 331–376
- [12] Woosley S E, Heger A and Weaver T A 2002 *Reviews of Modern Physics* **74** 1015–1071
- [13] Mönchmeyer R, Schaefer G, Müller E and Kates R E 1991 A&A **246** 417–440
- [14] Epstein R 1978 ApJ **223** 1037–1045
- [15] Burrows A and Hayes J 1996 Phys. Rev. Lett. **76** 352–355 (*Preprint* astro-ph/9511106)
- [16] Müller E and Janka H T 1997 A&A **317** 140–163
- [17] Yokozawa T, Asano M, Kayano T, Suwa Y, Kanda N, Koshio Y and Vagins M R 2014 *ArXiv e-prints* (*Preprint* 1410.2050)
- [18] Anderson W G, Brady P R, Creighton J D and Flanagan É É 2001 Phys. Rev. D **63** 042003 (*Preprint* gr-qc/0008066)